HAL
open science

UV-A-a photocatalytic degradation of the radionuclide complexants tributylphosphate and dibutylphosphat

E. Drinks, C. Lepeytre, C. Lorentz, M. Dunand, S. Mangematin, F. Dappozze, C. Guillard

To cite this version:

E. Drinks, C. Lepeytre, C. Lorentz, M. Dunand, S. Mangematin, et al.. UV-A-a photocatalytic degradation of the radionuclide complexants tributylphosphate and dibutylphosphat. Chemical Engineering Journal, 2018, 352, pp.143-150. 10.1016/j.cej.2018.06.120 . cea-02339829

HAL Id: cea-02339829

https://cea.hal.science/cea-02339829v1

Submitted on 5 Nov 2019

HAL is a multi-disciplinary open access archive for the deposit and dissemination of scientific research documents, whether they are published or not. The documents may come from teaching and research institutions in France or abroad, or from public or private research centers.

L'archive ouverte pluridisciplinaire **HAL**, est destinée au dépôt et à la diffusion de documents scientifiques de niveau recherche, publiés ou non, émanant des établissements d'enseignement et de recherche français ou étrangers, des laboratoires publics ou privés.

UV-A photocatalytic degradation of the radionuclide complexants tributylphosphate and dibutylphosphate

E. Drinks[a,b], Celia Lepeytre[b], C. Lorentz[a], F. Dappozze[a], Chantal Guillard*[a]

[a] Université Lyon 1, CNRS, UMR 5256, IRCELYON, Institut de Recherches sur la Catalyse et l'Environnement de Lyon, 2 avenue Albert Einstein, F-69626 Villeurbanne.

[b] CEA, DEN, DE2D, SEAD, Laboratoire des Procédés Supercritiques et de Décontamination BP 17171, F-30207 Bagnols-sur-Cèze, France

**Corresponding author: chantal.guillard@ircelyon.univ-lyon1.fr*

Email addresses:

Abstract

In this study, we evaluate and compare the photocatalytic degradation and mineralization of two alkylphosphates, tributylphosphate (TBP) and dibutylphosphate (DBP), in the presence of TiO_2 and under ultraviolet A radiation. Tri- and dibutylphosphate are used as extractants in nuclear decontamination processes and thus could be found in reprocessing plant waste water. We have investigated the degradation of TBP by gas chromatography–mass spectrometry, the fate of phosphate ions by ^{31}P NMR and ion chromatography, the mineralization kinetics of TBP and DBP by total organic carbon measurements, and finally, the formation of carboxylic acid by high-performance liquid chromatography with ultraviolet detection. Our results show that DBP is an intermediate product of the degradation of TBP and that the same types of carboxylic acids are formed during the degradation of both compounds. We also show that the

kinetics of the mineralization process is well described in both cases by the Langmuir-Hinshelwood model, with identical rate constants.

Keywords

Tributylphosphate, dibutylphosphate, photocatalysis, 31P NMR, carboxylic acid

1 Introduction

The approach most commonly used to reprocess spent nuclear fuel involves three steps: a mechanical step, a dissolution step, and then liquid/liquid separation using a specific extractant [1]. In the conventional PUREX (Plutonium and Uranium Refining by EXtraction) chemical treatment process, uranium, plutonium, other actinides and most of the fission products are dissolved in a nitric acid solution. Uranium and plutonium are then separated and purified using tributylphosphate (TBP) as an extractant. This extractant is diluted using an organic compound, hydrogenated tetrapropylene in France [2].

The cycles of extraction and back extraction steps yield purified uranium and plutonium nitrates and after conversion, the resulting plutonium oxide is used to prepare uranium and plutonium MOX (mixed oxide) fuel. The nitric acid, extractant and solvent used in these processes have to be recycled and the liquid and gaseous effluents and solid waste have to be managed. Furthermore, the irradiation of TBP during the extraction process by the actinides and fission products, leads to the formation of radiolysis products, namely dibutylphosphate (DBP), monobutylphosphate, organic acids and butanol [3, 4]. Therefore, the secondary liquid waste could contain residual TBP and DBP, which can cause emulsification and act as actinide complexants. Tributylphosphate is also used in other industries, as an extractant for rare earth elements, in aircraft hydraulic fluid [5, 6], as a plasticizer and flame retardant for vinyl resins [7], as a wetting agent in the textile and paper industries, and as an anti-foaming agent.

The decontamination of liquid waste containing TBP and its degradation species is therefore a common industrial problem.

Tributylphosphate is a refractory molecule particularly difficult to degrade. The most promising results have been obtained using ultraviolet (UV) C radiation and TiO_2 nanoparticles in the presence of H_2O_2 [8-10]. This photocatalytic process follows first order kinetics [8-10] and allows a 400 mg/L solution of TBP to be totally degraded in 70 min, and a 240 mg/L solution of DBP in roughly 45 min. The present study investigated the degradation of TBP and DBP by TiO_2 photocatalysis using UV-A irradiation. The degradation process was followed by recording the solution concentrations of residual carbon and phosphate ions, measured respectively by total organic carbon (TOC) analysis and ion chromatography. The appearance and disappearance of carboxylic acids, intermediate compounds in the reaction, was also monitored. To our knowledge, this article is the first to demonstrate TBP and DBP degradation using UV-A radiation and the first to provide a mechanistic explanation of the mode of degradation.

2 Experimental details

2.1 Materials

2.1.1 Photocatalysts

Photocatalytic experiments were performed using commercial (Degussa) P-25 TiO_2 nanoparticles with an 80/20 anatase/rutile ratio (diameter, 20–30 nm; density, 3.8 g/cm^3; specific surface area, about 50 m^2/g).

2.1.2 Chemical products

Tri- and dibutylphosphate (99 and 97% purity, respectively) were purchased from Sigma-Aldrich and used as received. All the aqueous solutions used in this study were prepared using ultra-pure water with a resistivity of 18.2 MΩ·cm.

2.2 Photoreactor and light sources

All experiments were carried out in a 1 L cylindrical glass reactor containing a central 125 W Philips HPK lamp inside a Pyrex tube. A jacket with circulating water was placed around the Pyrex tube to absorb IR radiation and thus prevent any heating of the solutions. The use of Pyrex glass ensured that < 290 nm radiation was blocked. The solutions were mixed constantly using a magnetic stirrer placed at the bottom of the reactor.

2.3 Procedure

The TiO_2 nanoparticles (375 mg) were added to 750 mL of aqueous solutions of TBP or DBP at different concentrations. The TiO_2 concentration (0.5 g/L) was chosen to ensure all the incident photons were absorbed. All reactions were conducted at room temperature, using ambient air as oxidant. The suspensions were kept under magnetic stirring to ensure adequate mixing and contact between the nanoparticles and the organic molecules. Before irradiation, the solutions were kept in the dark for 2 h under stirring to reach adsorption equilibrium between the pollutant and the photocatalyst. Samples were regularly withdrawn: 8 mL for gas chromatography–mass spectrometry (GC/MS), TOC, and carboxylic acid analyses, 5 mL for ion chromatography. The 8 mL samples were directly filtered through 0.45 µm Millipore filters to remove the TiO_2 particles. The 5 mL samples were basified at pH 13 using NaOH before filtration to desorb the phosphate ions from the surface of the photocatalyst.

2.4 Analytical Measurements

The overall efficiency of the process was determined by measuring the decrease in the concentration of total organic carbon using a Shimadzu TOC-VCPN analyzer equipped with an auto-sampler. The concentration of TBP was also measured by GC/MS using a DB-5MS capillary GC column (length, 30 m; inner diameter, 0.25 mm × 0.25 µm). The temperature conditions were 250°C for injection, 280°C for the detector, and the oven was initially kept at

50°C for 1 min, raised to 160°C at 10°C/min, then raised up to 270°C and kept at this temperature for 5 min. The helium flow was 1.3 mL/min and the mass spectrometer was operated in electron impact ionization mode at 70 eV.

The formation of phosphate ions was followed by ion chromatography using a Dionex DX-120 device and an AS14A (250 mm x 4 mm) column. The flow rate was 1.2 mL/min. The mobile phase consisted of 84 mg of $NaHCO_3$ and 848 mg of Na_2CO_3 per liter of pure water. The injection volume was 50 µl.

The formation of carboxylic acids was monitored by high-performance liquid chromatography with ultraviolet detection using a Waters 600 pump, a Waters 486 UV detector (detection at 210 nm), and a Transgenomic COREGel 87H3 7.8 mm (300 mm × 7.8 mm) column. The flow rate was 0.7 mL/min. The injection volume was 50 µL and the mobile phase was H_2SO_4 (5×10^{-3} mol/L).

Liquid-state ^{31}P-NMR analyses of the photocatalytic degradation of aqueous solutions of 100 ppm of TBP or DBM were performed by mixing 400 ml of solution irradiated for different times in 200 ml of D_2O. The experiments were performed on a Bruker Avance HD 400 spectrometer equipped with a 5 mm Bruker BBFO probe, operating at a ^{31}P Larmor frequency of 161.97 MHz. The initial delay was 2 s and the 90° pulse length was 7.85 µs.

3 Results and discussion

3.1 Photocatalytic degradation of TBP

3.1.1 Disappearance

We first confirmed that the concentration of TBP in the solution did not decrease under direct irradiation at wavelengths above 300 nm without TiO_2 (photolysis, data not shown). Fig. 1 shows that TBP disappears completely from the solutions when both TiO_2 and

of UV irradiation are present, indicating a purely photocatalytic process. The initial disappearance rate of TBP under these conditions was found to be 6 µmol/L/min.

` The photonic efficiency, $\rho = r/\phi$, is the ratio of the reaction rate, r, the number of reactant molecules converted per second, and the incident flux of efficient photons, ϕ (i.e. the ones absorbable by the TiO_2 nanoparticles). Considering the number of photons emitted per second (290 nm (0.8 mW/cm2) + 365 nm (3.2 mW/cm2) and assuming all the photons are absorbed by the photocatalyst, this gives a photonic efficiency of 0.6%. This value is of the same order as those reported in the literature for the photocatalytic degradation of other aqueous pollutants [11].

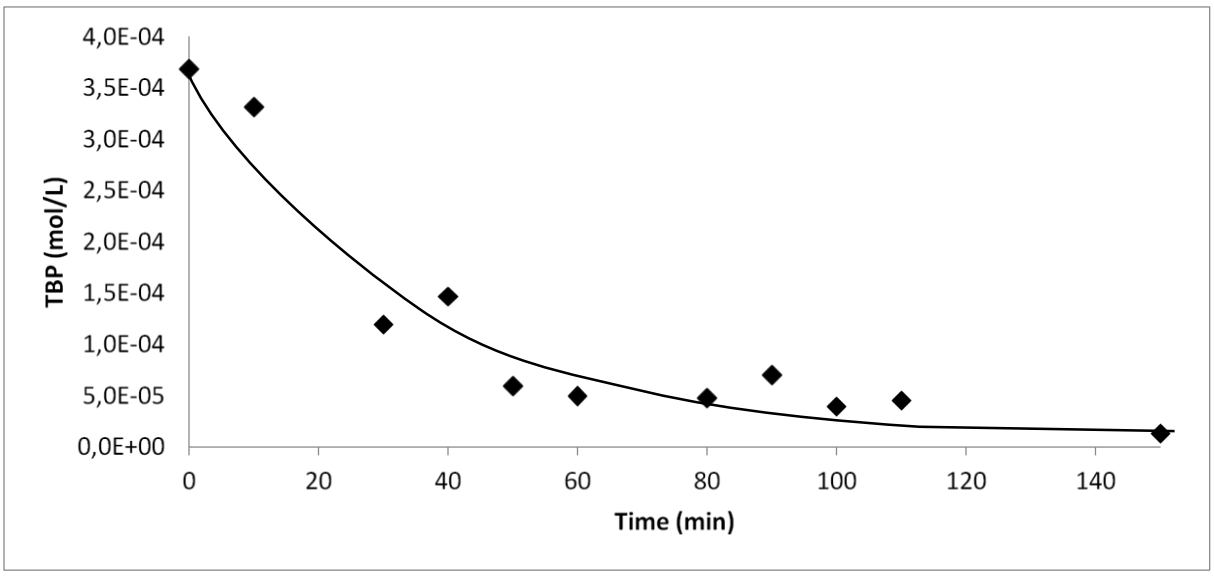

Fig. 1. Photocatalytic degradation of a solution of tributylphosphate (TBP) at an initial concentration of 3.9×10^{-4} mol/L under UV-A irradiation and in the presence of 0.5 g/L TiO_2 nanoparticles.

3.1.2 Variation of the pH during the degradation of TBP

Fig. 2 shows that the pH of the solution decreases rapidly in the initial stages of the TiO_2-assisted photodegradation of TBP, dropping from 6.8 to about 3.5. This drop in pH indicates that acidic species are formed. A pH of ca. 3.5 is expected given the initial TBP

concentration if the phosphorus compounds are completely mineralized and transformed into phosphoric acid. Our results therefore suggest that H_3PO_4 is formed from the phosphonate groups. The transient formation of aliphatic acids may also contribute to the drop in pH, but to a lesser extent.

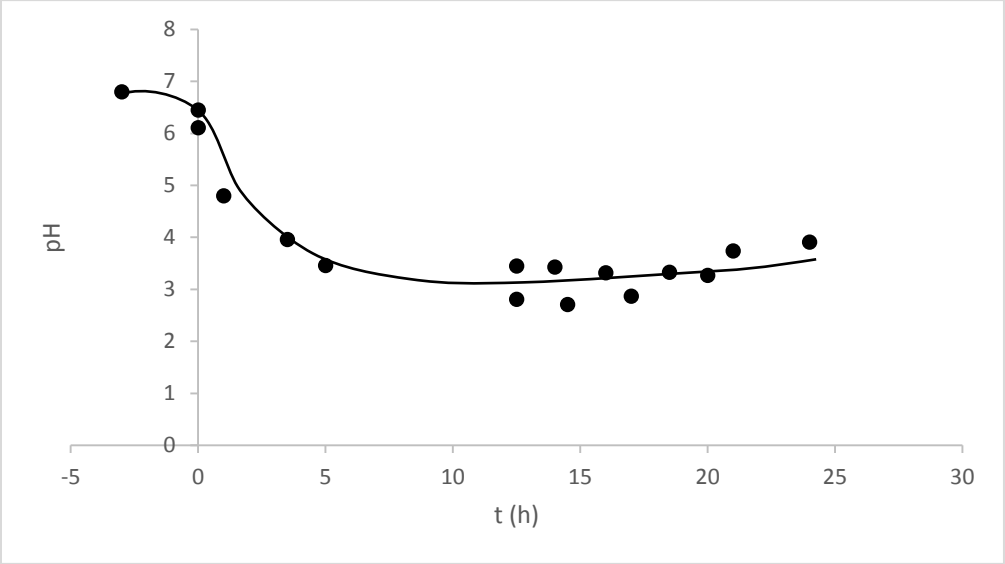

Fig. 2. Variation of pH as a function of UV-A irradiation time in an aqueous solution of tributylphosphate containing 0.5 g/L TiO_2 nanoparticles.

3.1.3 Fate of the phosphorus atoms

Fig. 3 shows that phosphate ions do not immediately appear following the disappearance of TBP, indicating that the formation of phosphate ions is not the first step in the degradation process. After disappearance of TBP only small amounts of phosphorus are transformed into phosphate ions indicating that the majority of organic compounds still contain phosphorus. After about 15 h, more than 95% of the phosphorus atoms are mineralized into phosphate ions (Fig. 3).

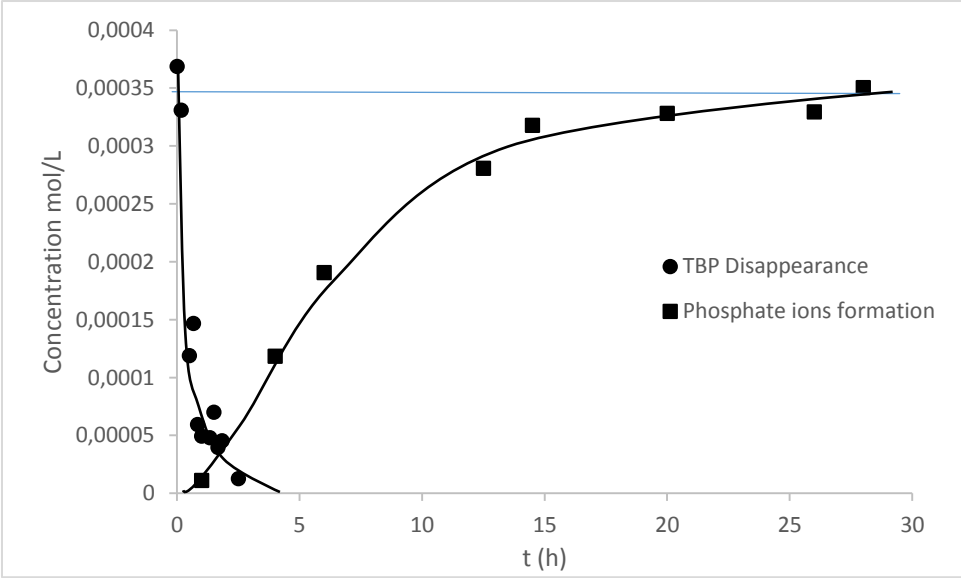

Fig. 3. Concentration of tributylphosphate and phosphate ions as a function of time in a solution with an initial concentration of 3.8×10^{-4} mol/L tributylphosphate (100 ppm) under UV-A irradiation and in the presence of 0.5 g/L TiO_2 nanoparticles.

The ^{31}P NMR spectra in Fig. 4 show the peak from TBP at −0.16 ppm, and three new peaks that appear as TBP degrades, at −0.92 ppm, 2.53 ppm and 3.74 ppm, which are respectively assigned to DBP, $H_2PO_4^-$, and an unidentified organic phosphate compound.

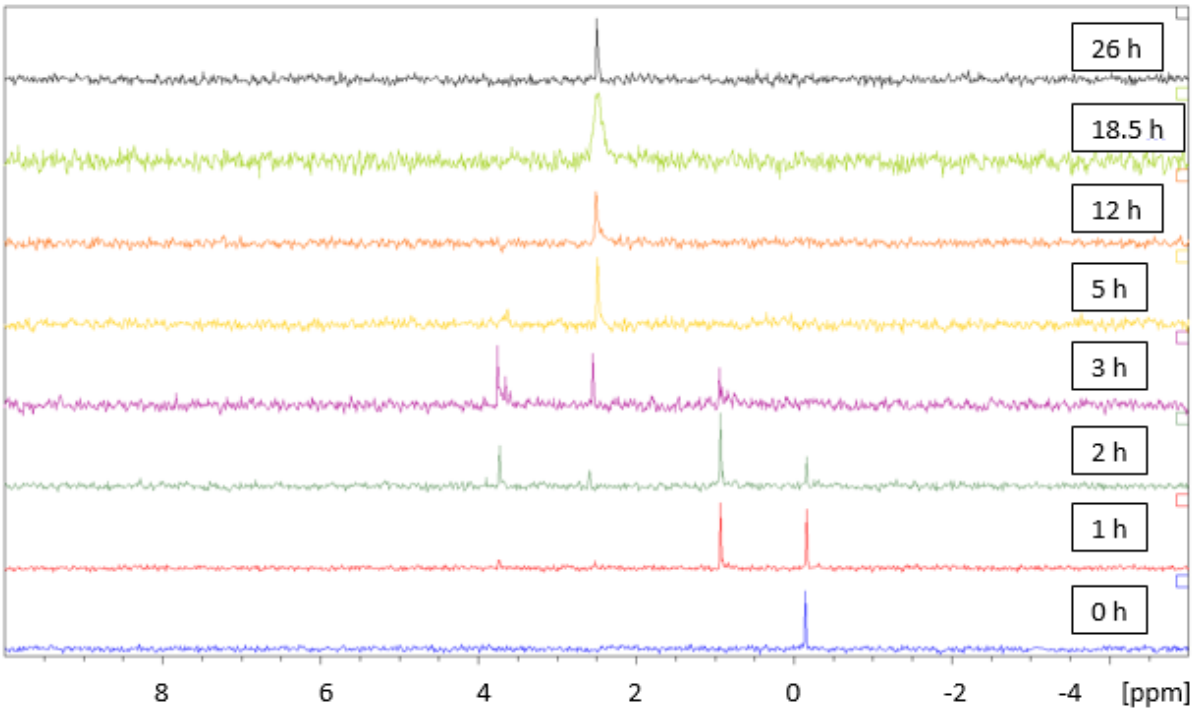

Fig. 4. ^{31}P NMR spectra acquired at different stages of the degradation of a solution of 3.8×10^{-4} mol/L tributylphosphate (100 ppm; corresponding to 4.5×10^{-4} mol/L carbon) under UV-A irradiation and in the presence of 0.5 g/L TiO_2 nanoparticles.

The DBP peak appears after 1 h of irradiation along with trace peaks from $H_2PO_4^-$ and the unidentified organic phosphate. Subsequently, the latter two peaks increase in intensity while the DBP peak weakens. At 3 h of irradiation, new peaks appear next to the one from the unidentified compound and remain until 5 h of irradiation. Beyond 12 h of irradiation, only the $H_2PO_4^-$ peak is observed.

3.1.4 Mineralization

Fig. 5 shows the decrease in the TOC concentration as a function of time for three solutions with initial concentrations of between 4×10^{-4} mol/L and 5×10^{-5} mol/L TBP, highlighting the mineralization of TBP by photocatalysis.

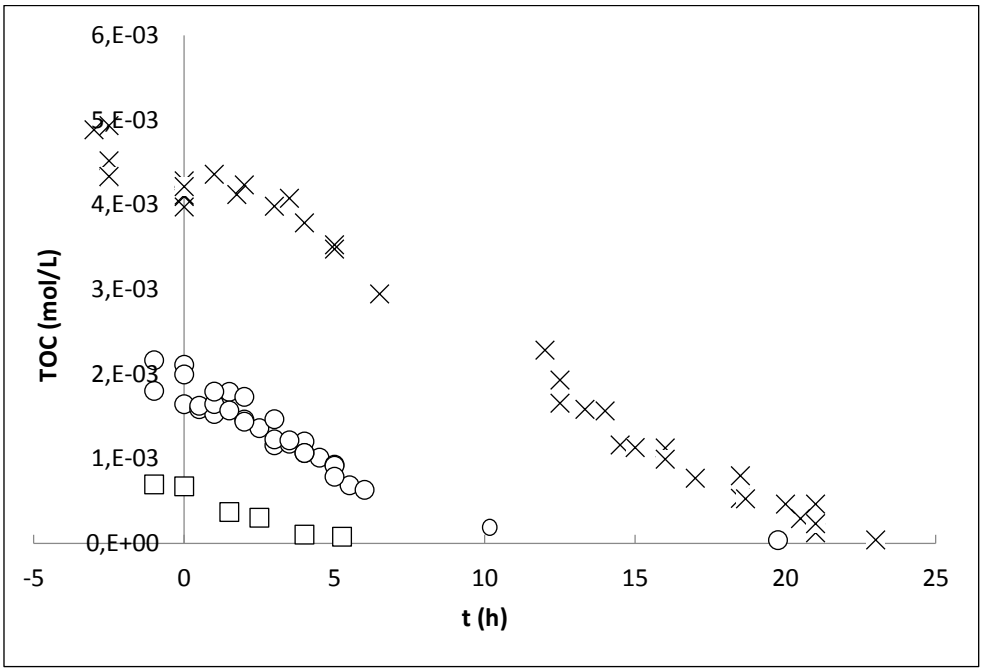

Fig. 5. Evolution of the total organic carbon (TOC) concentration as a function of the UV-A irradiation time for tributylphosphate solutions at 3.8×10^{-4} mol/L, 1.7×10^{-4} mol/L, and 5.8×10^{-5} mol/L containing 0.5 g/L TiO_2 nanoparticles.

The decrease in the TOC concentration as the irradiation time increases shows that the carbon atoms from TBP are transformed into CO_2. Comparing these results with those shown in Fig. 3 reveals that the TOC only starts to decrease substantially several hours after the TBP has completely disappeared. In the solution with an initial TBP concentration of 3.8×10^{-4} mol/L for instance, more than 95% of the organic carbon is still present after 5 h of irradiation. This indicates that the first steps of the degradation involve either the oxidation of the carbonated chain and/or the breaking up of TBP. The appearance of DBP (Fig. 4) suggests that TBP does indeed break up. At the lowest concentration of TBP, the TOC concentration decreases more rapidly, suggesting that the surface of the TiO_2 nanoparticles was not saturated.

3.1.5 Formation of carboxylic acid

Fig. 6 shows the concentrations of different carboxylic acids measured by HPLC during the degradation of a TBP solution under UV-A irradiation. Six types of acid were detected in total, namely 2-Ketobutyric acid ($CH_3CH_2COCOOH$), propionic acid (CH_3CH_2COOH), lactic acid ($CH_3CHOHCOOH$), pyruvic acid ($CH_3COCOOH$), acetic acid and formic acid. Other compounds with higher retention times were also observed. They were not identified but do not correspond to alcohols, aldehydes, ketones or other carboxylic acids with four carbon atoms or fewer. It is probably that these compounds contained phosphorous atoms.

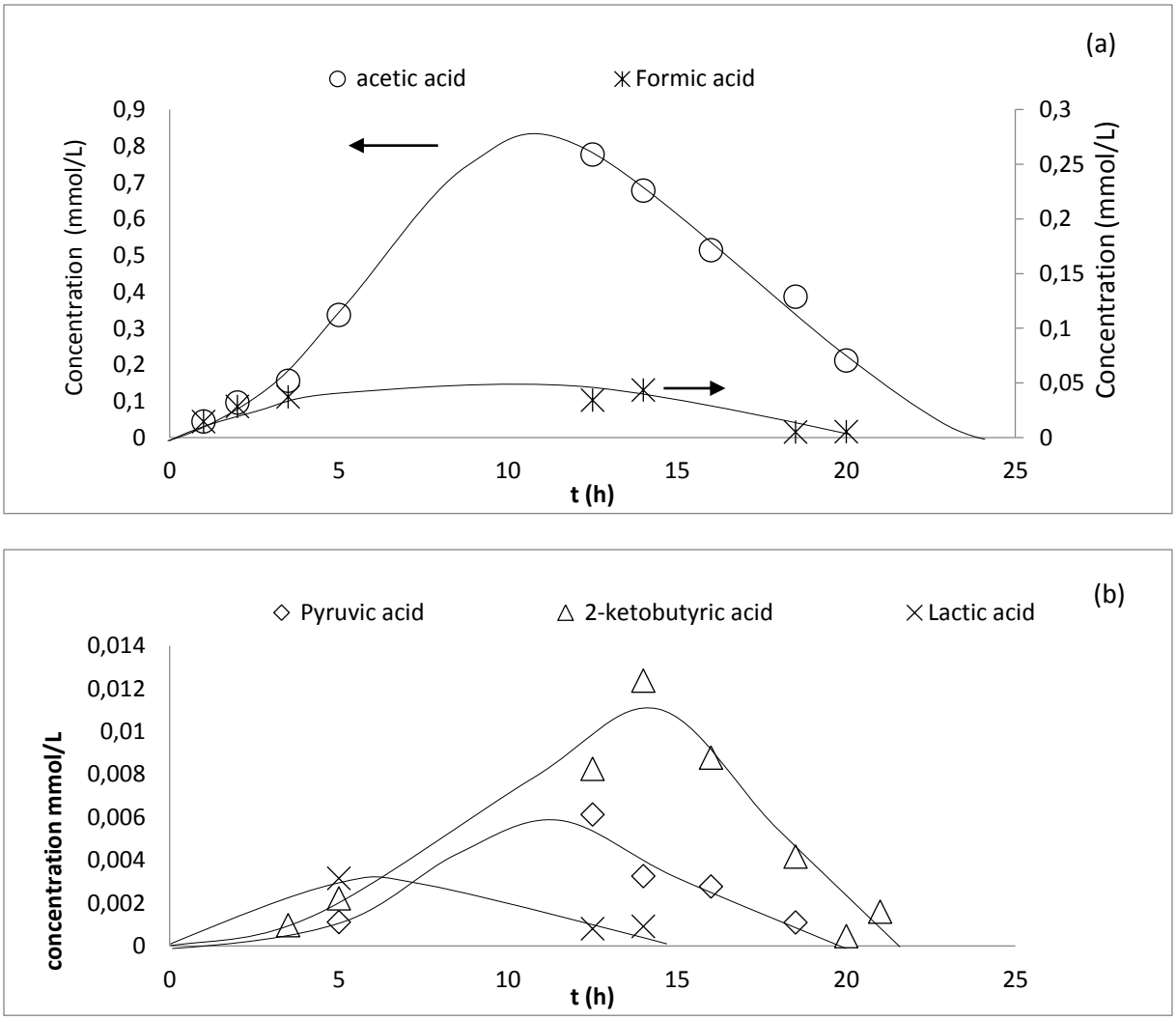

Fig. 6. Formation of (a) acetic and formic acid and (b) pyruvic acid, 2-ketobutyric acid and lactic acid during the photocatalytic degradation (UV-A irradiation, 0.5 g/L TiO_2 nanoparticles) of a 4.07×10^{-4} mol/L solution of tributylphosphate.

Trace amounts of propionic acid are only detected after 20 h of irradiation. This late arrival suggests that it is a product of the decarboxylation of 2-ketobutyric acid:

$$CH_3\text{-}CH_2\text{-}CO\text{-}COOH + ½\ O2 \rightarrow CH_3CH_2COOH + CO_2 \quad (1)$$

Since the concentrations of lactic acid, pyruvic acid and acetic acid peak at different times, our interpretation is that lactic acid is progressively degraded by oxidation to form pyruvic acid, which is then decarboxylated to form acetic acid:

$$CH_3\text{-}CHOH\text{-}COOH + ½\ O2 \rightarrow CH_3\text{-}CO\text{-}COOH \rightarrow CH_3COOH + CO_2 \quad (2)$$

However, the amount of acetic acid formed during the reaction (Fig. 6a) indicates that this is not the only mechanism through which it is formed. The fact that acetic acid is the carboxylic acid that reaches the highest concentration during the reaction may be explained by its reactivity toward hydroxyl radicals (1.6×10^7 L/mol/s), which is about 100 times less than those of other carboxylic acids [12].

Fig. 7 shows the concentrations of organic carbon in the form of carboxylic acid and the total concentration in the solution at different irradiation times. At 5 h, carboxylic acids account for about a third of the TOC present in solution, and after 20 h of irradiation of the TBP solution, all the organic carbon is in the form of carboxylic acids.

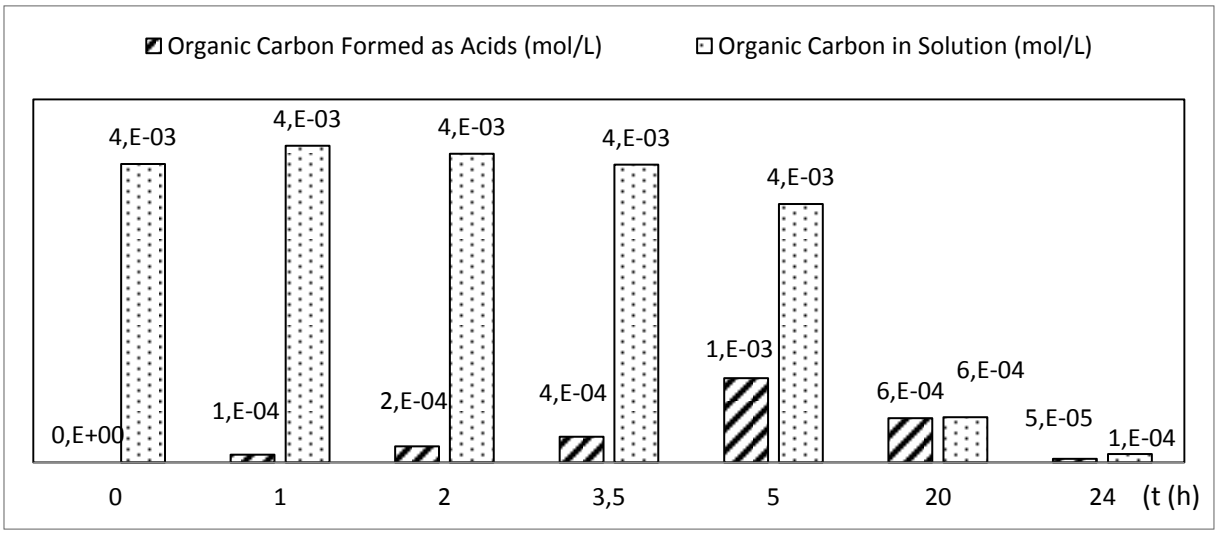

Fig. 7. Total concentrations of organic carbon in the solution and concentration in the form of carboxylic acids as a function of UV-A irradiation time in a tributylphosphate solution with an initial concentration of 4×10^{-4} mol/L in the presence of 0.5 g/L TiO_2 nanoparticles.

3.2 Comparison of the photocatalytic degradation of TBP and DBP

The photocatalytic degradation of alkylphosphate compounds in general was investigated by comparing those of TBP and DBP. This was achieved by comparing the disappearance of organic carbon, the fate of phosphate ions by ^{31}P NMR, and the formation of carboxylic acids.

3.2.1 Comparison of the mineralization of TBP and DBP

Fig. 8a shows the time required to photocatalytically degrade more than 99% of the carbon in solutions of TBP and DBP with different initial concentrations. Fig. 8b shows the corresponding average rates of carbon elimination. The time required to degrade more than 99% of the TOC increases linearly with the initial concentration of the pollutant and does not depend on its nature. At the same TOC concentration, the time required to remove more than 99% of the TOC is similar for TBP and DBP. Fig. 8b shows that the average mineralization rate increases linearly with the initial carbon concentration before reaching a plateau at concentrations greater than 4×10^{-3} mol/L.

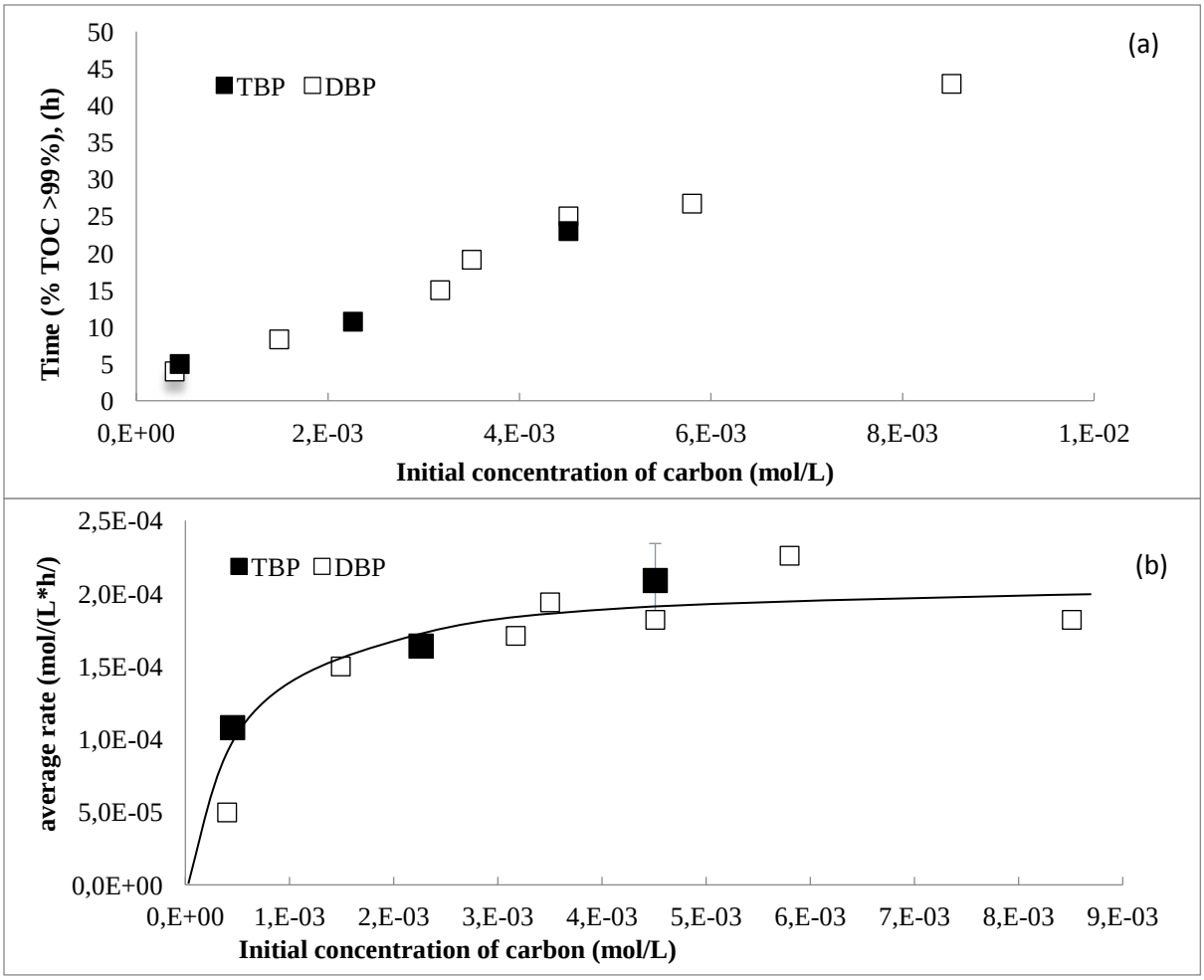

Fig. 8. (a) Time taken to remove 99% of the total organic carbon from solutions of tri- and dibutylphosphate and (b) the corresponding average rates of disappearance, both as a function of the initial concentration of carbon in the solutions (4×10^{-4} mol/L tributylphosphate corresponds to 4.81×10^{-3} mol/L carbon; 5.631×10^{-4} mol/L dibutylphosphate corresponds to 4.51×10^{-3} mol/L carbon). The solutions were irradiated with UV-A light and contained 0.5 g/L TiO_2 nanoparticles.

This curve is typical of a Langmuir-Hinshelwood process, in which the reaction rate is given by:

$$r = \frac{k * K * C}{1 + (K * C)}$$

where k is the rate constant of the reaction and K is the equilibrium (or adsorption) constant. The rate constants and adsorption constants calculated using these data for TBP and DBP are identical, within experimental errors ($k \approx 2.2 \times 10^{-4}$ mol/L/h and $K \approx 0.45 \times 10^{3}$ L/mol).

3.2.2 Comparison of the fate of phosphate ions during TBP and DBP degradation.

Fig. 9 shows ^{31}P NMR spectra acquired at different times during the photocatalytic degradation of a DBP solution with a carbon content (4.8×10^{-3} mol/L) similar to that of the TBP solution whose spectra are shown in Fig. 4.

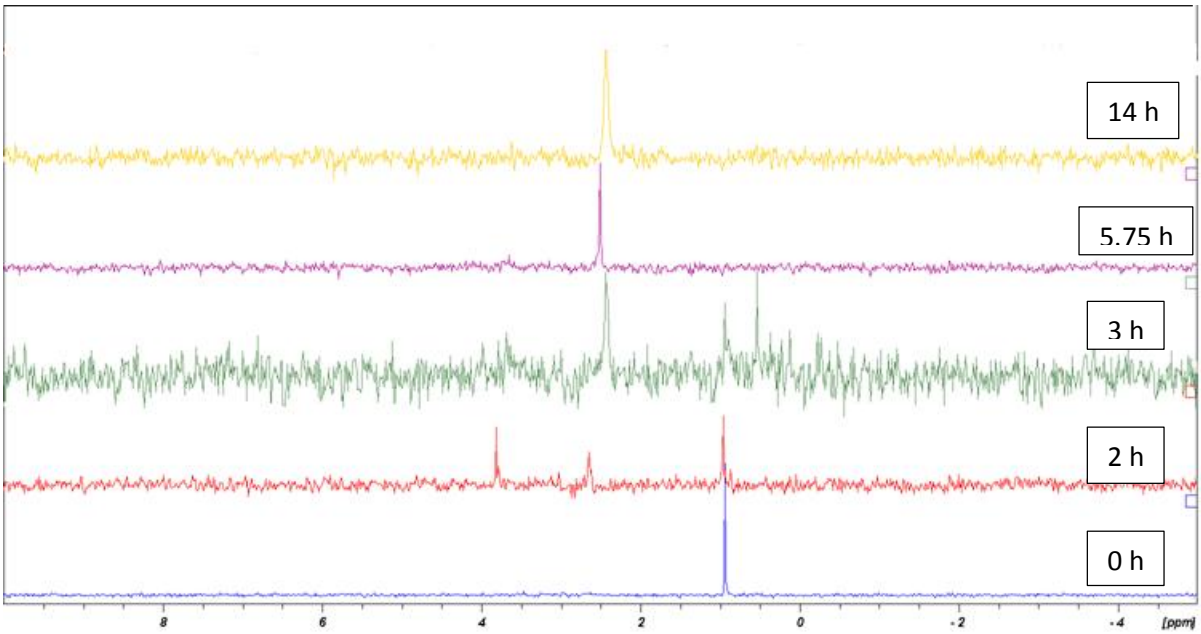

Fig. 9. ^{31}P NMR spectra acquired at different stages of the degradation of a solution of 5.63×10^{-4} mol/L (100 ppm) dibutylphosphate, corresponding to 4.51×10^{-3} mol/L carbon, under UV-A irradiation, in the presence of 0.5 g/L TiO_2 nanoparticles.

The DBP peak is detected at 0.92 ppm and as observed for the TBP solution, peaks from $H_2PO_4^-$ (at 2.53 ppm) and the same unidentified phosphate compound (at 3.74 ppm) appear during degradation. Considering that DBP is formed from TBP, this suggests that the

unidentified compound is monobutylphosphate. After 3 h of irradiation, a new peak appears at 0.55 ppm, not observed during the degradation of TBP, along with a weaker, broader signal at 3.7 ppm that also appears in the corresponding TBP spectrum (Fig.4, 3 h). After 5.75 h, only $H_2PO_4^-$ is detected.

In summary, this ^{31}P NMR analysis shows that during the degradation of DBP, an unidentified organic compound containing a phosphorus atom (resonating at 0.55 ppm) forms that is not detected during the degradation of TBP. The other unidentified peaks at 3.74 ppm and the weak shoulder at 3.74 ppm are also observed during the degradation of TBP. Further work is required to identify these two compounds.

3.2.3 Comparison of the carboxylic acids formed during the degradation of TBP and DBP.

Fig. 10 shows how the concentrations of different carboxylic acids vary as a function of irradiation time during the degradation of a 4.1×10^{-4} mol/L solution of DBP, and during the degradation of an equivalent solution of TBP. The same carboxylic acids are formed for both alkylphosphates.

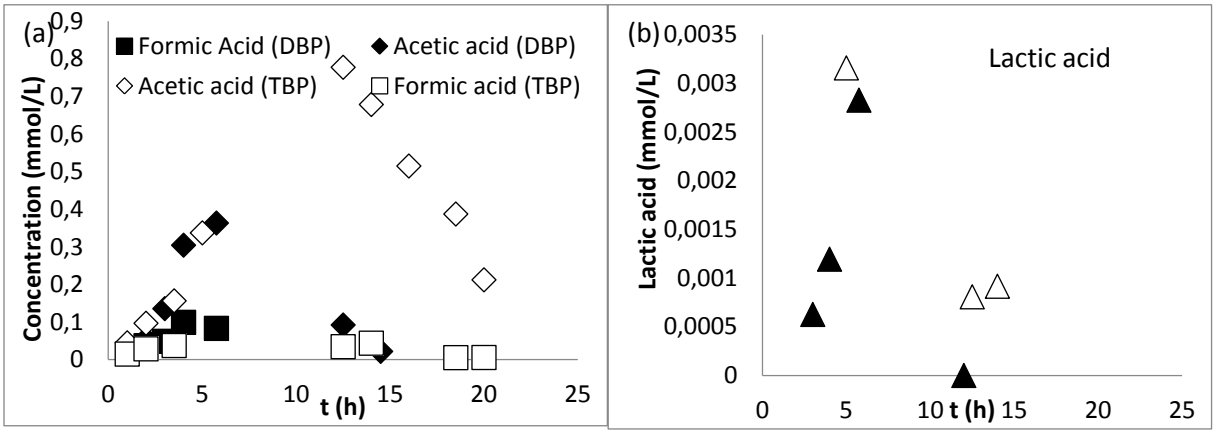

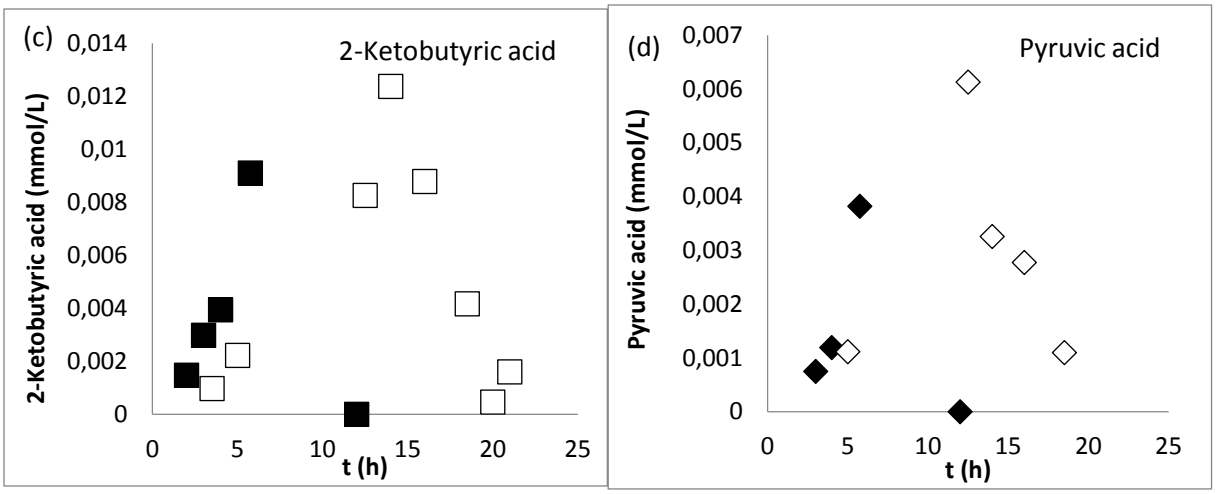

Fig. 10. Comparison of the time evolutions of the concentrations of carboxylic acids during the photocatalytic degradation of 4.1×10^{-4} mol/L solutions of dibutylphosphate (filled symbols) and tributylphosphate (blank symbols) under UV-A radiation and in the presence of 0.5 g/L TiO_2 nanoparticles.

Acetic acid is the carboxylic acid that reaches the highest concentration during the degradation of both alkylphosphates, because of its low reactivity with hydroxyl radicals [12]. The maximum concentrations measured for all the carboxylic acids are lower for the DBP solution and they disappear sooner than from the TBP solution, which is consistent with the lower carbon content of DBP.

4 Conclusions

The present study demonstrates for the first time that TBP and DBP can be mineralized using non-damaging radiation (UV-A), with an irradiance similar to that of solar light (4 mW/cm^2) and without adding an oxidant.

Our results show that less than 10% of the TOC of the solution has disappeared at the time all the TBP has degraded, indicating that the first steps in this process are the oxidation of the alkyl chain and/or the breaking of the bond between the phosphate and the alkyl group. The

latter is confirmed by ^{31}P NMR spectra showing that DBP is formed during the degradation of TBP. The NMR data also show that similar phosphorus compounds form during the degradation of DBP and TBP, one of which is probably monobutylphosphate.

Analysis of the TOCs of solutions of TBP and DBP at different concentrations suggest that both mineralization process have identical Langmuir-Hinshelwood kinetics. The average carbon disappearance rate and the time required to remove 99% of the organic carbon are directly proportional to the initial carbon content of the solution.

The same carboxylic acids are formed during the degradation of TBP and DBP, namely 2-ketobutyric acid, lactic acid, pyruvic acid, formic acid, and acetic acid, the latter being the one found in the highest concentration because of its low reactivity with hydroxyl radicals. These carboxylic acids only appear once the alkylphosphates have completely disappeared. Pyruvic acid arises from the oxidation of lactic acid and is then transformed into acetic acid. In keeping with the smaller number of carbon atoms in DBP than in TBP, smaller amounts of carboxylic acids are formed during the degradation of DBP. Finally, our data also show that before being evacuated as CO_2, all the organic carbon in the solution is in the form of carboxylic acids.

Acknowledgments

The authors thank ORANO inc. for financial support and Stephane Mangematin for help with the GC/MS analysis.

References

[1] Y.Z. Wei, Progress and Discussion on Chemical Separation Technologies for Nuclear Fuel Reprocessing Developed Abroad, Prog. Chem. 23 (2011) 1272–1288.

[2] A. Dodi, G. Verda, Improved determination of tributyl phosphate degradation products (mono- and dibutyl phosphates) by ion chromatography, J. Chromatogr. A 920 (2001) 275–281.

[3] D.D. Dicholkar, L.K. Patil, V.G. Gaikar, S. Kumar, U.K. Mudali, R. Natarajan, Direct determination of tri-n-butyl phosphate by HPLC and GC methods, J. Radioanal. Nucl. Chem. 291 (2012) 739–743.

[4] Y. Gao, W.F. Zheng, X.M. Cao, S.L. Chen, Studies on Pu-238 induced alpha radiolysis of the solvent TBP, J. Radioanal. Nucl. Chem. 303 (2015) 377–383.

[5] X.P. Ouyang, B.Q. Fan, H.Y. Yang, R. Qing, Research on Air Content Estimation of Tributyl Phosphate Hydraulic Fluids: A Novel Approach Based on the Vacuum Method, J. Dyn. Syst. Meas. Control. 136 (2014) 024503.

[6] A. Marklund, B. Andersson, P. Haglund, Traffic as a source of organophosphorus flame retardants and plasticizers in snow, Environ. Sci. Technol. 39 (2005) 3555–3562.

[7] C. Katsoulis, E. Kandare, B.K. Kandola, The combined effect of epoxy nanocomposites and phosphorus flame retardant additives on thermal and fire reaction properties of fiber-reinforced composites, J. Fire Sci. 29 (2011) 361–383.

[8] M.J. Watts, K.G. Linden, Photooxidation and subsequent biodegradability of recalcitrant tri-alkyl phosphates TCEP and TBP in water, Water Res. 42 (2008) 4949–4954.

[9] H. Seshadri, P.K. Sinha, Photocatalytic performance of combustion synthesized beta-Ga2O3 for the degradation of tri-n-butyl phosphate in aqueous solution, J. Radioanal. Nucl. Chem. 292 (2012) 649–652.

[10] H. Seshadri, K. Kumar, M. Garg, P. Velavendan, S. Ganesh, P.K. Sinha, Synthesis, characterization and evaluation of nanocrystalline anatase titania for the degradation of dibutyl phosphate, J. Radioanal. Nucl. Chem. 300 (2014) 157–162.

[11] D. Gregori, C. Guillard, I. Benchenaa, D. Leonard, S. Parola, Hybrid sol–gel porous nanocomposites as efficient photocatalyticcoatings: Insights in the structure/reactivity relationships, Appl. Catal. B 176 (2015) 472–479

[12] G.V Buxton, C.L.Greenstock, W.P.Helman, A.B.Ross, Critical Review of rate constants for reactions of hydrated electrons, hydrogen atoms and hydroxyl radical in aqueous solution, J. Phys. Chem. Ref. Data 17 (1988) 513–886.